Neuron
Article

Temporal Target Restriction of Olfactory Receptor Neurons by Semaphorin-1a/PlexinA-Mediated Axon-Axon Interactions

Lora B. Sweeney,[1,3] Africa Couto,[2,4] Ya-Hui Chou,[1,4] Daniela Berdnik,[1] Barry J. Dickson,[2] Liqun Luo,[1,*] and Takaki Komiyama[1,3,5]
[1] Howard Hughes Medical Institute, Department of Biological Sciences and Neurosciences Program, Stanford University, Stanford, CA 94305, USA
[2] Research Institute of Molecular Pathology (IMP), A-1030 Vienna, Austria
[3] These authors contributed equally to this work.
[4] These authors contributed equally to this work.
[5] Present address: Janelia Farm Research Campus, Howard Hughes Medical Institute, Ashburn, VA 20147, USA.
*Correspondence: lluo@stanford.edu
DOI 10.1016/j.neuron.2006.12.022

SUMMARY

Axon-axon interactions have been implicated in neural circuit assembly, but the underlying mechanisms are poorly understood. Here, we show that in the *Drosophila* antennal lobe, early-arriving axons of olfactory receptor neurons (ORNs) from the antenna are required for the proper targeting of late-arriving ORN axons from the maxillary palp (MP). Semaphorin-1a is required for targeting of all MP but only half of the antennal ORN classes examined. Sema-1a acts nonautonomously to control ORN axon-axon interactions, in contrast to its cell-autonomous function in olfactory projection neurons. Phenotypic and genetic interaction analyses implicate PlexinA as the Sema-1a receptor in ORN targeting. Sema-1a on antennal ORN axons is required for correct targeting of MP axons within the antennal lobe, while interactions amongst MP axons facilitate their entry into the antennal lobe. We propose that Sema-1a/PlexinA-mediated repulsion provides a mechanism by which early-arriving ORN axons constrain the target choices of late-arriving axons.

INTRODUCTION

Specific molecular recognition between pre- and postsynaptic neurons is generally thought to be the primary mechanism by which connection specificity is established in the nervous system. However, axon-axon interactions among input neurons or dendrite-dendrite interactions among target neurons could further contribute to connection specificity. This is particularly plausible in neural circuits in the central brain where axons from many input neurons form highly specific connections with many target neurons in a highly compact space. Indeed, axon-axon interactions have been implicated in the assembly of visual and olfactory circuits in flies and mammals (Brown et al., 2000; Clandinin and Zipursky, 2000; Ebrahimi and Chess, 2000; Feinstein and Mombaerts, 2004; Komiyama et al., 2004). However, neither the underlying molecular mechanisms of axon-axon interactions nor the cellular and developmental context under which such interactions take place are well understood.

The adult olfactory system of *Drosophila* contains ~50 classes of olfactory receptor neurons (ORNs), each expressing 1–2 specific odorant receptors and projecting their axons to one of 50 glomerular targets in the antennal lobe (Figure 1A). In contrast to the mouse olfactory system where odorant receptors themselves have instructive information about ORN targeting specificity (Mombaerts et al., 1996; Wang et al., 1998; Imai et al., 2006), odorant receptors in *Drosophila* do not play a role in this process (Dobritsa et al., 2003). Although several molecules have been shown to be required for aspects of axon targeting of *Drosophila* ORNs (Ang et al., 2003; Hummel et al., 2003; Hummel and Zipursky, 2004; Jhaveri et al., 2004; Komiyama et al., 2004), mechanisms that instruct the target choice of individual ORN classes are largely unknown (reviewed in Komiyama and Luo [2006]).

At the antennal lobe, ORN axons form highly specific synaptic connections with dendrites of second-order olfactory projection neurons (PNs), most of which send dendrites to a single glomerulus. Previous studies have shown that PN dendritic targeting is specified by lineage, birth order, and intrinsic transcriptional control (Jefferis et al., 2001; Komiyama et al., 2003), and initial targeting occurs prior to the arrival of pioneering ORN axons in the antennal lobe (Jefferis et al., 2004). When ORN axons start to invade the antennal lobe, a coarse map in the protoantennal lobe has already formed by virtue of specific PN dendrite targeting (Jefferis et al., 2004). Given this developmental sequence, ORN axon targeting in principle could recognize cues on PN dendrites or non-PN cues at the antennal lobe, or they could self-organize through axon-axon

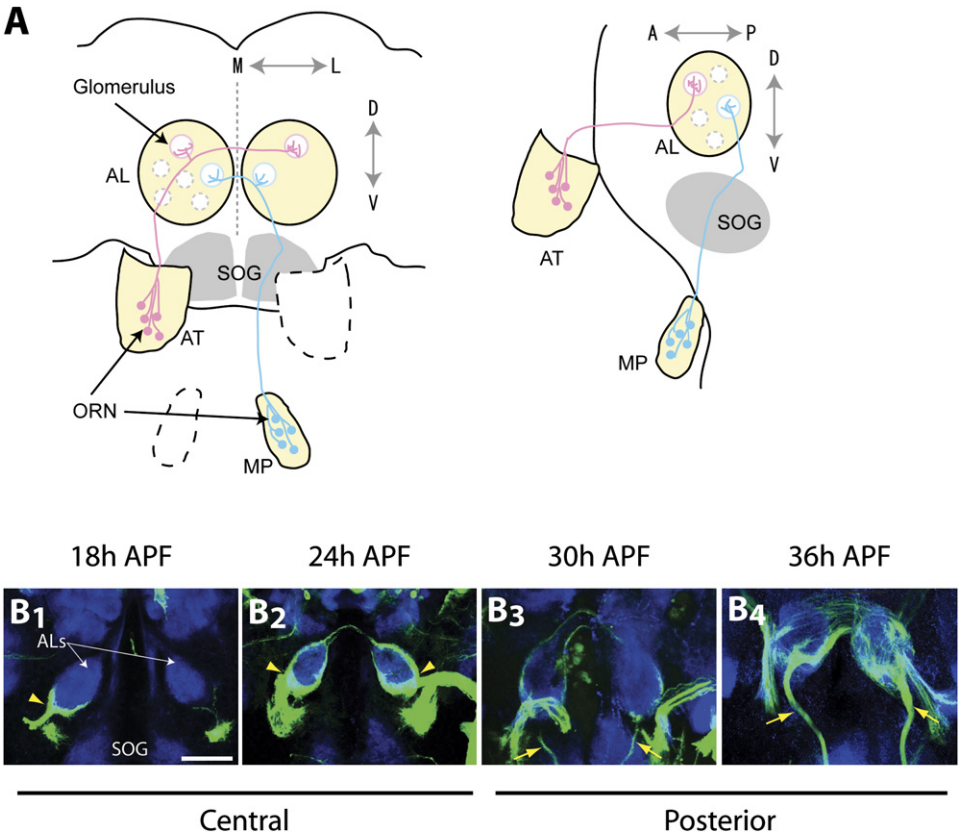

Figure 1. Antennal ORN Axons Reach the Developing Antennal Lobe before MP ORN Axons

(A) Schematic of the organization of the *Drosophila* olfactory system (Left, frontal view; Right, sagittal view). AT, antenna; MP, maxillary palp; AL, antennal lobe; SOG, suboesophageal ganglion; A, anterior; P, posterior; D, dorsal; V, ventral; M, medial; L, lateral. Not drawn to scale.

(B) Pioneering antennal ORN axons (arrowheads) arrive at the developing antennal lobe at 18 hr after puparium formation (APF), whereas pioneering MP ORN axons (yellow arrows) reach the antennal lobe at 30–32 hr APF. The central (left panels) or posterior (right panels) section of the antennal lobe is shown. Green, mCD8-GFP marking ORN axons, maximum-intensity confocal stack *z*-projections; blue, N-cadherin (18 hr and 24 hr panels) or Sema-1a (30 hr and 36 hr panels) immunostaining, single confocal sections. Genotype: *elav-Gal4 eyFLP; FRTG13 tubP-Gal80/FRTG13 UAS-mCD8GFP*. Scale bar, 50 μm.

interactions. We provide an example and mechanism for the self-organization strategy in this study.

Evidence for the use of axon-axon interactions in *Drosophila* ORN axon targeting came from a previous study of the POU transcription factor Acj6 (Komiyama et al., 2004). Genetic mosaic analyses indicated that Acj6 function in some ORNs is required for the correct axon targeting of other ORNs. This observation implies the existence of hierarchical interactions among different ORN classes (Komiyama et al., 2004). However, it is unclear how such interactions take place: which classes interact and what molecules mediate these interactions. Here, we show that early-arriving antennal ORN axons are required for targeting fidelity of late-arriving maxillary palp (MP) ORN axons. We further provide molecular mechanisms of this axon-axon interaction among ORNs: Semaphorin-1a (Sema-1a) in antennal ORNs acts as a ligand for MP ORNs to restrict their target choice, and this signaling is most likely mediated through its repulsive receptor PlexinA. Our study provides a molecular, cellular, and developmental context of how axon-axon interactions are used for regulating ORN axon targeting specificity.

RESULTS

Maxillary Palp ORN Axons Reach the Antennal Lobe after Antennal Axons

Approximately 1200 *Drosophila* ORNs reside in each third segment of the antenna, whereas ~120 ORNs reside in each MP. Individual ORNs from most antenna and MP classes target their axons to a single glomerulus in the ipsi- as well as the contralateral antennal lobe (Stocker, 1994; Figure 1A). It has previously been shown that pioneering ORN axons from the antenna arrive at the periphery of the developing antennal lobe around 18 hr after puparium formation (18 hr APF) (Jhaveri et al., 2000; Jefferis et al., 2004). To determine when MP axons reach the developing antennal lobe, we selectively visualized ORN axons using eyFLP MARCM in combination with panneural

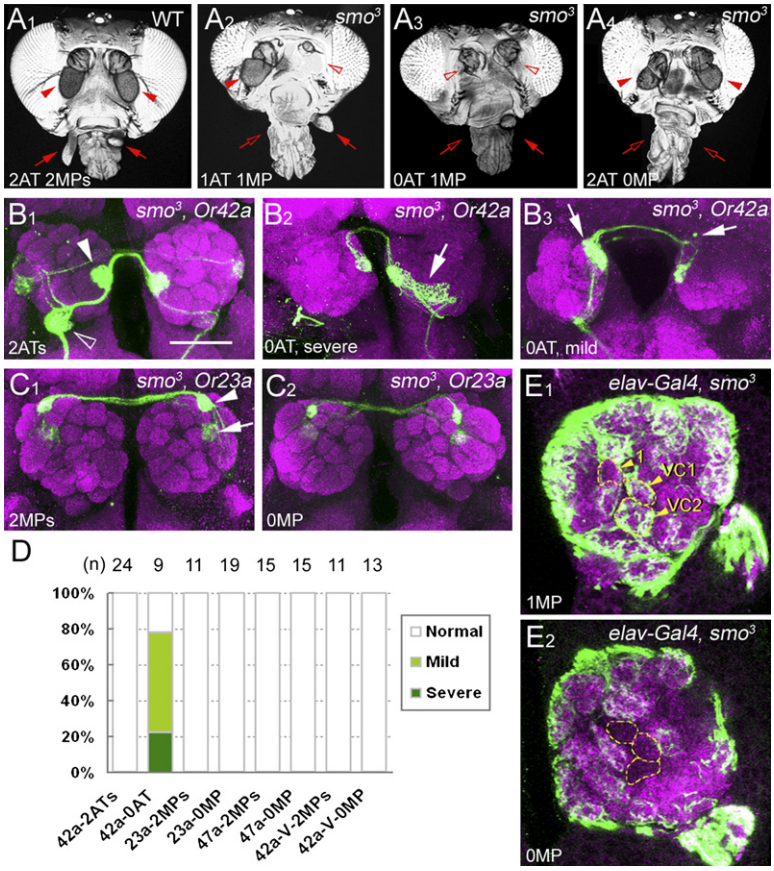

Figure 2. Antennal ORN Axons Are Required for Targeting Fidelity of MP ORN Axons

(A) Occasional loss of antenna(e) or maxillary palp(s) as a result of eyFLP-induced *smoothened* clones. (A_1) A control adult head has two antennae (AT) and two maxillary palps (MP). (A_2–A_4) Examples of adult heads of eyFLP-induced *smo*^{3} MARCM flies that are missing one or both antenna(e) or MP(s), as indicated. Antennae and MPs are indicated by arrowheads and arrows, respectively. Open arrowheads and open arrows mark missing third antennal segment(s) and MP(s), respectively.

(B) In eyFLP-induced *smo*^{3} MARCM flies, Or42a axons from the MP target correctly to the VM7 glomeruli in flies containing one (data not shown) or both antennae (filled arrowhead in [B_1]). In flies lacking both antennae (0 AT), Or42a axons cluster extensively in ventral-medial glomeruli (arrow in [B_2]) or ectopically project to dorsal-medial antennal lobe (arrows in [B_3]).

(C) In eyFLP-induced *smo*^{3} MARCM flies, Or23a ORN axons from the antenna project to DA3 (arrowhead) and DC3 (arrow) correctly in flies having both (C_1) or no (C_2) MP.

(D) Quantification of axon-targeting phenotypes of one MP and three antennal ORN classes under conditions when different sensory organs are missing. Or23a- and Or42a-Gal4 label axons that target to more than one glomeruli, possibly a consequence of incomplete *cis*-regulatory sequences used in these Or-Gal4 transgenes (see Table 1). Or42a-V represents antennal ORNs that ectopically expressed *Or42a-Gal4* resulting in the labeling of ORNs targeting to the glomerulus V (open arrowhead in [B_1]).

(E) All *smo*$^{-/-}$ ORNs are labeled in green by a panneural *elav*-Gal4 driver in conjunction with eyFLP MARCM. In the antennal lobe of a fly with one intact MP (E_1), ORN axons innervate normal MP axon target glomeruli VC2, VC1, 1 (arrowheads), as well as VA4, VA7l, and VM7 (data not shown; in different confocal sections). In the antennal lobe of a fly with no MP (E_2), these MP target glomeruli are no longer innervated by any green axons, indicating that antennal ORN axons do not invade these MP axon-free glomeruli (yellow dashed circles and data not shown). n = 12 and 10 for 1 MP and 0 MP samples, respectively.

Scale bar, 50 μm (B and C). Genotype: (A_1) *UAS-mCD8GFP eyFLP FRT19A/+; tubP-Gal80 FRT40A/CyO.* (A_2–A_4) *UAS-mCD8GFP eyFLP FRT19A/+; smo*^{3} *FRT40A/tubP-Gal80 FRT40A.* (B–D): *UAS-mCD8GFP eyFLP FRT19A/+; smo*^{3} *FRT40A/tubP-Gal80 FRT40A; Or-Gal4/+.* (E) *UAS-mCD8GFP eyFLP FRT19A/elav-Gal4 hsFLP UAS-mCD8GFP; smo*^{3} *FRT40A/tubP-Gal80 FRT40A*.

elav-Gal4 (Jefferis et al., 2004) every 2 hr from 18 to 36 hr APF (Figure 1B; data not shown).

After leaving the proboscis and entering the brain, MP axons travel dorsally through the suboesophageal ganglion (SOG) neuropil and enter the antennal lobe from a ventral posterior position. Thus, MP ORN axons can be unequivocally distinguished from the antennal ORN axons, which enter the antennal lobe from a lateral and anterior position (Figure 1A; Figure 1B, yellow arrowheads and arrows, respectively, for antennal and MP ORN axons). We found that the first MP axons reach the developing antennal lobe between 30 and 32 hr APF (Figure 1B_3). By 36 hr APF, pioneering MP axons enter the antennal lobe and cross to the contralateral side (Figure 1B_4). Prior to MP ORN axon arrival at 30–32 hr APF, axons from antennal ORNs have surrounded the entire periphery (Figures 1B_2 and 1B_3; data not shown) and have begun to penetrate into the antennal lobe (Hummel and Zipursky, 2004; Jefferis et al., 2004). This temporal difference in the arrival of these two groups of ORN axons led us to hypothesize that antennal axons direct MP axons to their proper target area.

Antennal ORN Axons Are Required for Targeting Fidelity of MP Axons

To test whether antennal ORN axons are required for correct targeting of MP axons, we made use of a serendipitous observation that generation of *smoothened* (*smo*) null clones using eyFLP results in the occasional loss of one or both third antennal segment(s) or maxillary palp(s), thus eliminating the population of ORNs within (Figure 2A). This is presumably caused by the fact that Hedgehog signaling is essential for early eye-antennal disc proliferation (Cho et al., 2000). In animals with two intact antennae,

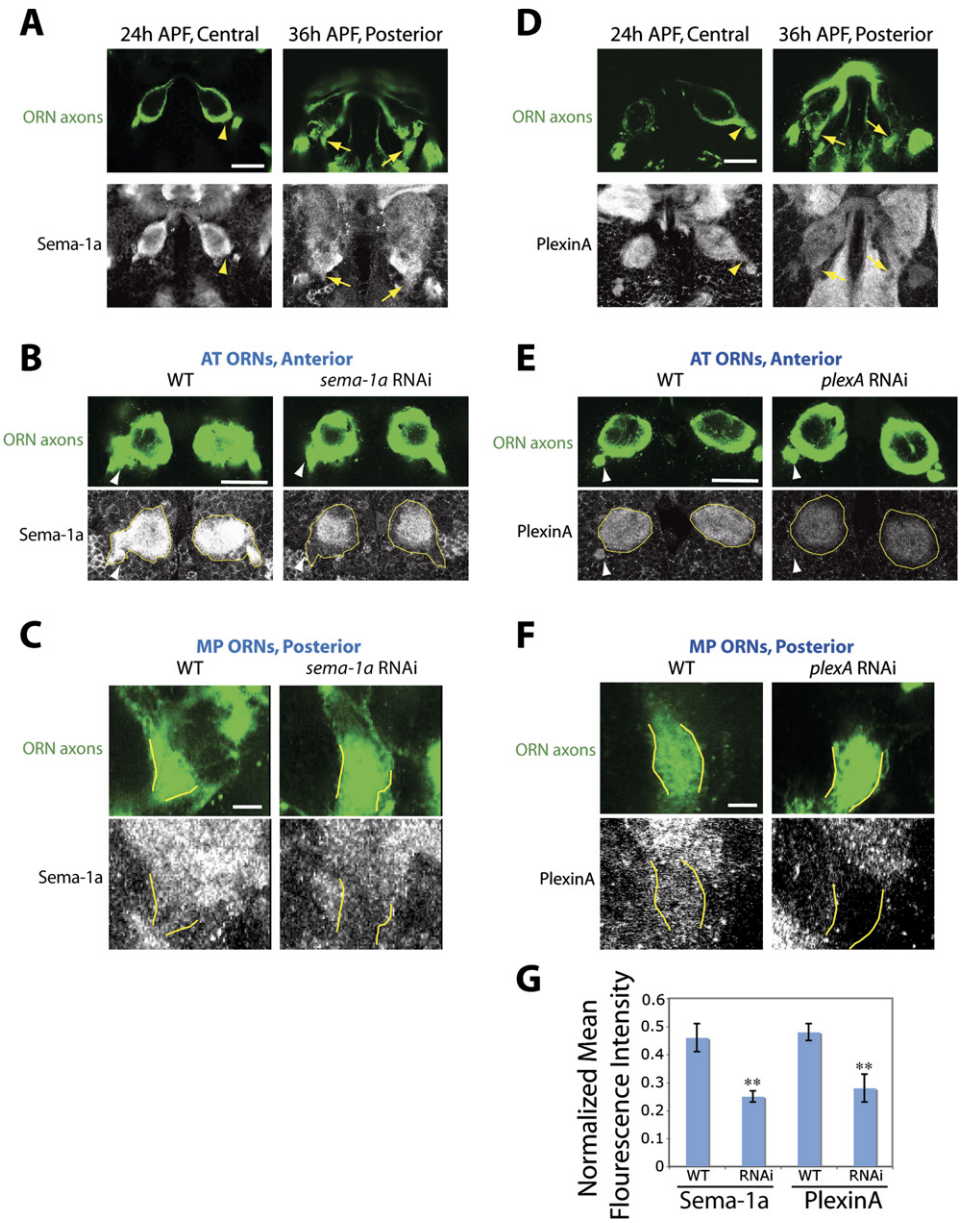

Figure 3. Expression of Sema-1a and PlexinA in Antennal and MP ORN Axons

(A) Sema-1a is expressed in ORN axons from the antenna (arrowheads; central section of the antennal lobe) and MP (arrows; posterior section of the antennal lobe) at 24 hr and 36 hr APF, respectively. At 24 hr APF, Sema-1a staining is much stronger in the ORN layer than PN dendrites in the center of the antennal lobe. Green, mCD8-GFP as a marker for ORN axons; white, Sema-1a.

(B) UAS-*sema-1a* RNAi driven by *pebbled*-Gal4 results in a marked reduction of the Sema-1a protein in the ORN axon layer of the anterior antennal lobe (yellow outline) and antennal axon bundles (arrowheads). Twenty-five hours APF at 29°C (roughly equivalent to 34 hr APF at 25°C). Green, mCD8-GFP as a marker for ORN axons; white, Sema-1a.

(C) UAS-*sema-1a* RNAi driven by *pebbled*-Gal4 results in a significant reduction of the Sema-1a protein in MP axons in the posterior antennal lobe (yellow outline). Twenty-five hours APF at 29°C. Note that Sema-1a expression domain is wider than the MP bundle, suggesting that other neighboring neuronal processes that are *pebbled*-Gal4 negative also express Sema-1a. Green, mCD8-GFP marking ORN axons; white, Sema-1a.

(D) PlexinA is expressed in ORN axons from the antenna (arrowheads, central antennal lobe section) and MP (arrows, posterior antennal lobe section) at 24 hr and 36 hr APF, respectively. Green, mCD8-GFP as a marker for ORN axons; white, PlexinA.

(E) UAS-*plexinA* RNAi driven by *pebbled*-Gal4 results in a marked reduction of the PlexinA protein in the ORN axon layer of the anterior antennal lobe (yellow outline) and antennal axon bundles (arrowheads). Twenty-five hours APF at 29°C. Green, mCD8-GFP as a marker for ORN axons; white, PlexinA.

(F) UAS-*plexinA* RNAi driven by *pebbled*-Gal4 results in a marked reduction of the PlexinA protein in MP axons in the posterior antennal lobe (yellow outline). Twenty-five hours APF at 29°C. Green, mCD8-GFP marking ORN axons; white, PlexinA.

axons from *smo*$^{-/-}$ MP ORNs expressing Or42a correctly target to their normal glomerulus (Figure 2B$_1$), indicating that *smo* itself does not affect targeting of this MP ORN class. By contrast, when both antennae failed to form in 9 of ~8000 flies screened (e.g., Figure 2A$_3$, open arrowheads), Or42a expressing axons mistarget in seven of nine cases (Figures 2B$_2$ and 2B$_3$; quantified in Figure 2D). The axons often mistarget to areas normally occupied by antennal ORN axons. The strong correlation between the loss of both antennae (including all antennal ORN axons) and MP axon targeting defects indicates that antennal ORN axons contribute to the fidelity of MP axon targeting. Conversely, loss of both MPs did not affect axon targeting of three antennal ORN classes examined (Figures 2C$_1$ and 2C$_2$ and Figure 2D), suggesting that antennal ORN axons do not require MP axons for correct targeting.

In principle, antennal ORN axons could influence MP axon targeting indirectly through their postsynaptic targets such as the PNs. For example, lack of ORN innervation could disrupt PN dendritic organization, in turn causing other ORNs to mistarget. Alternatively, PN dendrites lacking their antennal presynaptic partners could attract the available MP ORN axons, causing them to mistarget. Several lines of evidence argue against these possibilities. First, PN dendrites target to their appropriate areas and create a protomap independent of ORN axons (Jefferis et al., 2004) and can refine even when ORN axon invasion into the antennal lobe is severely disrupted (Zhu and Luo, 2004). Second, we have recently shown that at least in the adult, wiring specificity of the olfactory system is extremely stable. ORN axons do not invade neighboring glomeruli devoid of ORN axons as a result of specific ORN ablation (Berdnik et al., 2006). Third, in the cases when both MPs are missing (e.g., Figure 2A$_4$, open arrows), antennal ORN axons do not invade the unoccupied MP glomerular targets (Figure 2E). Thus, the most likely interpretation of MP axon mistargeting in the absence of antennal axons is that antennal axons normally guide the targeting of MP axons directly.

To further elucidate the mechanisms by which ORNs interact with each other, we searched for molecules that govern ORN axon targeting. Two sets of experiments led to the identification of Sema-1a and PlexinA, a ligand and receptor pair known to regulate embryonic motor axon guidance (Kolodkin et al., 1993; Winberg et al., 1998; Yu et al., 1998), as candidate molecules required for ORN axon targeting. First, in a directed genetic approach, we found that Sema-1a plays a critical role in ORN axon targeting (see below). Second, in an unbiased transgenic RNAi screen (A.C. and B.J.D., unpublished data), we found that an ORN-specific knockdown of Sema-1a and PlexinA resulted in ORN targeting defects. In the rest of this study, we explore the mechanisms by which Sema-1a-PlexinA signaling between ORN axons controls their targeting.

Expression of Sema-1a and PlexinA in ORN Axons

We first characterized the expression of Sema-1a and PlexinA in ORN axons. We used an antibody specific to Sema-1a (Yu et al., 1998) to stain the developing antennal lobe. The antibody specificity was further confirmed by a drastic reduction of Sema-1a staining in pupal brains when a UAS-RNAi transgene against *sema-1a* was driven by a panneural Gal4 line (see Figure S1A in the Supplemental Data available with this article online); this experiment also indicates that the majority of Sema-1a in the pupal brain is made by neurons. We found that Sema-1a is highly expressed in antennal ORN axons in the developing antennal lobe from 18–36 hr APF (Figure 3A, arrowheads; data not shown). In a separate study, we showed that Sema-1a is also expressed in PN dendrites prior to ORN axon arrival (Komiyama et al., 2007). However, after ORN axon arrival, the Sema-1a protein level is higher in the ORN axon layer at the periphery of the antennal lobe compared to the central antennal lobe where PN dendrites reside (Figure 3A, left). To confirm Sema-1a expression in ORN axons, we knocked down Sema-1a in ORNs by RNAi using *pebbled*-Gal4, which is expressed in all developing ORNs but not in cells in the brain near the antennal lobe (Figure S2). This resulted in a marked reduction of Sema-1a staining specifically in the ORN axon layer at the periphery of the antennal lobe (Figure 3B). At 36 hr APF, Sema-1a is also expressed in a bundle of axons between the SOG and ventral antennal lobe; this axon bundle includes MP axons when they approach the developing antennal lobe (Figure 3A, right; Figure 3C). *pebbled*-Gal4-driven UAS-*sema-1a* RNAi significantly reduced the Sema-1a immunofluorescence intensity in the MP ORN axon bundle (Figure 3C; quantified in Figure 3G), confirming Sema-1a expression in these axons.

To examine the expression pattern of PlexinA in the olfactory system, we raised a polyclonal antibody against PlexinA (see Experimental Procedures). Specificity of this affinity-purified antibody was verified by a marked reduction of PlexinA level in pupal brains when a UAS-*plexinA* RNAi transgene was driven by a panneural Gal4 (Figure S1B); this also indicates that the majority of PlexinA in the pupal brain is made by neurons. Using this antibody, we found that PlexinA is highly expressed in the developing antennal lobe including both antennal and MP ORNs (Figure 3D, arrowheads and arrows, respectively).

(G) Quantification of *pebbled*-Gal4 Sema-1a and PlexinA RNAi knockdown in MP ORN axons at 25 hr APF (29°C). From single confocal sections chosen from the green channel, mean fluorescence intensity of Sema-1a (left) and PlexinA (right) staining within MP axon bundles was quantified, normalized to the fluorescence intensity of a *pebbled*-negative region, and plotted. Error bar, SEM. For Sema-1a staining, n = 8 for both samples; for PlexinA staining, n = 10 and 7 for control and RNAi, respectively. $p < 0.01$ (t test) for both comparisons.

Scale bar, 50 μm (A, B, D, and E); 5 μm (C and F). Genotype: (A and D) *pebbled-Gal4; UAS-mCD8GFP*. (B and C) WT: *pebbled-Gal4 UAS-mCD8GFP*. RNAi: *pebbled-Gal4 UAS-mCD8GFP/UAS-sema-1a RNAi*. (E and F) WT: *pebbled-Gal4 UAS-mCD8GFP*. RNAi: *pebbled-Gal4 UAS-mCD8GFP; UAS-plexinA RNAi/+*.

Selective knockdown of PlexinA by *pebbled*-Gal4 in ORNs results in a drastic reduction of PlexinA level in the ORN axon layer at the periphery of the antennal lobe (Figure 3E), confirming the contribution of antennal ORN axons to PlexinA staining in the antennal lobe. At 36 hr APF, PlexinA expression is also found in the axon bundle between the SOG and ventral antennal lobe that includes the MP axon bundle. *pebbled*-Gal4 driven *plexinA* RNAi expression significantly reduced the PlexinA immunofluorescence intensity in the MP bundle (Figure 3F; quantified in Figure 3G), confirming that PlexinA is expressed on MP axons as they approach the developing antennal lobe.

In summary, these expression studies indicate that both Sema-1a and PlexinA are expressed in both antennal and MP axons at times when these axons reach the antennal lobe and begin to select their targets.

Sema-1a Is Required in ORNs for Axon Targeting of All MP but Only Half of Antennal ORN Classes

To test the function of Sema-1a in ORN axon targeting, we analyzed targeting of 17 different ORN classes using Or-Gal4 lines to label specific classes of ORN axons. These classes encompass about one third of all ORN classes in the adult *Drosophila*, including all sensillar types (Table 1). In the first two sets of experiments, we removed Sema-1a using the *sema-1a*^{P1} null allele (Yu et al., 1998) from about half or almost all ORNs using eyFLP MARCM or eyFLP/cell lethal strategies, respectively (Newsome et al., 2000; Hummel et al., 2003; Hummel and Zipursky, 2004; Komiyama et al., 2004; Zhu and Luo, 2004; Figures 4A$_1$ and 4A$_2$). In the MARCM strategy, only *sema-1a*$^{-/-}$ axons of a particular class are visualized by the Or-Gal4. In the eyFLP/cell lethal strategy, all ORN axons of one class are visualized, of which the vast majority are *sema-1a*$^{-/-}$. In both cases, cells in the central brain are heterozygous as eyFLP restricts recombination in the olfactory system to the peripheral organs (Hummel et al., 2003; Hummel and Zipursky, 2004; Komiyama et al., 2004; Zhu and Luo, 2004).

All five MP ORN classes examined exhibited severe axon-targeting defects (Figures 4B–4D and S3A). Often MP ORN axons fail to enter the antennal lobe and form extra-antennal lobe terminations. These de novo terminations are enriched for the presynaptic marker nc82 at the small space between the SOG and the ventral part of the antennal lobe (Figures 4B–4D, arrows; quantified in Table 1) or occasionally within the SOG (data not shown). MP axons that enter the antennal lobe mistarget to inappropriate areas and form ectopic terminations (Figures 4B–4D, arrowheads; quantified in Table 1; also see Figure 5B), occasionally not invading their correct glomeruli at all. These phenotypes are caused by errors in axon target selection, as labeling of clones using HA-synaptotagmin in addition to mCD8-GFP revealed that ectopic terminations are highly enriched for this presynaptic marker (Figure S4). These phenotypes are specific to the loss of Sema-1a, as a second, independent allele (*sema-1a*^{P2}) exhibited similar phenotypes (data not shown).

Of the 12 classes of antennal ORNs examined, five are not affected even with the eyFLP/cell lethal strategy where the vast majority of ORNs are *sema-1a*$^{-/-}$ (Figures 4E and S3B; Table 1). This indicates that Sema-1a in ORNs is not required for axon targeting of these ORN classes. Among the remaining seven classes, all except Or67b and Or47b ORNs exhibited mild but highly penetrant targeting defects: axons always innervate their correct glomeruli but often spread slightly beyond their correct glomeruli (Figures 4H and 4I and Figure S3C; Table 1). Or67b and Or47b ORNs also always innervate their correct glomeruli but occasionally mistarget to more distant regions of the antennal lobe as well (Figures 4F and 4G, arrowhead; Table 1). Antennal axons never form ectopic terminations outside the antennal lobes.

The *Drosophila* antenna contains several morphologically different sensillar classes (Stocker, 1994), which map to different parts of the antennal lobe (Couto et al., 2005; Fishilevich and Vosshall, 2005) and potentially serve different functions (de Bruyne et al., 1999, 2001; Hallem and Carlson, 2006). Interestingly, all unaffected ORN classes belong to the antennal basiconic sensillar group, whereas most mildly affected classes belong to the trichoid sensillar group (Table 1). The only coeloconic ORN class whose OR expression has been characterized (Or35a) was also mildly affected. The biological significance of this correlation is currently unclear. In summary, Sema-1a in ORNs is required differentially for the targeting of different classes. Because of their severe phenotypes, we focus our subsequent analyses primarily on the MP classes.

Sema-1a Is Required Non-Cell-Autonomously for MP Axon Targeting

Although Semaphorins are known as axon guidance ligands (Dickson, 2002), we have shown recently that Sema-1a acts as a receptor in PNs for their dendritic and axonal targeting (Komiyama et al., 2007). Sema-1a also acts as a receptor for mushroom body neurons (Komiyama et al., 2007) and photoreceptor axons (Cafferty et al., 2006). To distinguish whether Sema-1a acts cell autonomously as a receptor or non-cell-autonomously as a ligand for ORN axon targeting, we performed two additional sets of mosaic experiments. In the first set, we generated small clones using hsFLP-based MARCM and visualized *sema-1a*$^{-/-}$ axons (Figure 4A$_5$). We found that *sema-1a*$^{-/-}$ ORN axons targeted normally (Figures 4B$_5$–4D$_5$ compared to Figures 4B$_4$–4D$_4$; Figure S3A; Table 1), indicating that Sema-1a does not act cell autonomously. These results also confirmed that *sema-1a* heterozygosity does not affect ORN axon targeting. Nonautonomy was further supported by eyFLP reverse MARCM experiments (Figure 4A$_3$), in which labeled *sema-1a*$^{+/+}$ ORN axons exhibited targeting defects similar to *sema-1a*$^{-/-}$ ORN axons when both are in an environment in which half of the ORNs are *sema-1a*$^{-/-}$ (Figures 4B$_3$–4D$_3$ compared to Figures 4B$_1$–4D$_1$; Table 1). The non-cell-autonomous requirement of Sema-1a in ORNs strongly suggests that

Table 1. Quantification of Mistargeting Frequency for 17 ORN Classes in Various Mosaic Manipulations

ORN Class	Olfactory Organ	Glomerular target(s)[a]	eyFLP MARCM WT	eyFLP MARCM *sema-1a*$^{-/-}$	eyFLP/Cell Lethal *sema-1a*$^{-/-}$	eyFLP Reverse MARCM	hsFLP MARCM WT	hsFLP MARCM *sema-1a*$^{-/-}$
Intra-AL Ectopic Termination[b]								
Or85e	MP	VC1	0% (20)	31% (13)	80% (15)	53% (17)	0% (34)	0% (39)
Or46a	MP	VA7l/VA7m/VA5	0% (29)	91% (11)	43% (7)	46% (26)	0% (16)	0% (14)
Or42a	MP	VM7(V,VL2P)	0% (29)	56% (16)	38% (13)	53% (17)	0% (14)	0% (15)
Or59c	MP	1(VM7,VC2)	0% (13)	13% (23)	67% (12)	29% (14)	0% (22)	0% (22)
Or71a	MP	VC2	0% (23)	62% (13)	100% (7)	59% (27)	0% (8)	0% (17)
Or10a	AT-basiconic	DL1	0% (24)	0% (7)	0% (7)	n.d.	n.d.	n.d.
Or22a	AT-basiconic	DM2	0% (13)	0% (16)	0% (24)	n.d.	n.d.	n.d.
Or47a	AT-basiconic	DM3	0% (8)	0% (20)	0% (20)	n.d.	n.d.	n.d.
Or92a	AT-basiconic	VA2	0% (26)	0% (27)	0% (20)	n.d.	n.d.	n.d.
Gr21a	AT-basiconic	V	0% (7)	0% (21)	0% (13)	0% (47)	0% (28)	0% (48)
Or67b	AT-basiconic	VA3	0% (23)	11% (28)	41% (22)	5% (20)	0% (13)	0% (17)
Or43a	AT-trichoid	DA4l	0% (16)	n.d.	100% (20)	n.d.	n.d.	n.d.
Or83c	AT-trichoid	VA6,DA4m,DC3	0% (7)	n.d.	100% (15)	n.d.	n.d.	n.d.
Or88a	AT-trichoid	VA1d	0% (5)	n.d.	66% (34)	n.d.	n.d.	n.d.
Or23a	AT-trichoid	DC3,DA3	0% (26)	n.d.	100% (32)	n.d.	n.d.	n.d.
Or47b	AT-trichoid	VA1lm	0% (36)	n.d.	25% (12)	n.d.	n.d.	n.d.
Or35a	AT-coeloconic	VC3	0% (15)	n.d.	100% (25)	n.d.	n.d.	n.d.
Extra-AL Termination								
Or85e	MP	VC1	0% (46)	4% (25)	62% (26)	12% (34)	0% (20)	0% (78)
Or46a	MP	VA7l/VA7m/VA5	0% (39)	13% (16)	65% (17)	9% (33)	0% (19)	0% (14)
Or42a	MP	VM7(V,VL2P)	0% (48)	13% (31)	65% (34)	3% (33)	0% (28)	0% (30)
Or59c	MP	1(VM7,VC2)	0% (20)	20% (45)	50% (28)	12% (25)	0% (44)	0% (54)
Or71a	MP	VC2	0% (32)	29% (17)	50% (18)	4% (45)	0% (16)	0% (34)
All antennal ORN classes			0%	0%	0%	0%	0%	0%

Data are represented as phenotypic penetrance in percentage followed by the number of samples examined (n, in parentheses). See text for description of phenotypic severity. For intra-AL ectopic termination, n is the number of the brains examined; for extra-AL terminations, n is the number of MP axon bundles (2/brain) examined. n.d., not determined.

[a] Some Or-Gal4s label more than one glomeruli, possibly a consequence of incomplete *cis*-regulatory sequences used in Or-Gal4 transgenes.

[b] For MP ORN classes, the percentage of Intra-AL Ectopic Termination is an under-estimate since mutant MP axons often form extra-AL terminations and do not enter the AL.

Sema-1a acts as a ligand to direct ORN axon-axon interactions.

PlexinA in ORNs Is Required for Their Axon Targeting

PlexinA is a well-characterized repulsive receptor for Sema-1a in *Drosophila* embryonic motor axon guidance (Winberg et al., 1998; Terman et al., 2002). To test the requirement of PlexinA in ORN axon targeting, we examined individual classes of ORN axons when the PlexinA protein level is knocked down using *pebbled*-Gal4-driven *plexinA* RNAi expression. Qualitatively, all four MP classes examined display the two characteristic targeting defects of *sema-1a* mutants: occasional extralobe terminations ventral to the antennal lobe (arrows in Figure 5A; Figure S5A) and frequent intra-antennal lobe ectopic terminations (arrowheads in Figure 5A; Figure S5A). We further compared the phenotypes of *plexinA* RNAi and *sema-1a* mutants by defining six regions of frequent ectopic termination inside the antennal lobe (Figure 5B, top). The distributions of mistargeting among these six regions are similar for each ORN class under both conditions (Figure 5B, bottom). These results support the idea that Sema-1a and PlexinA

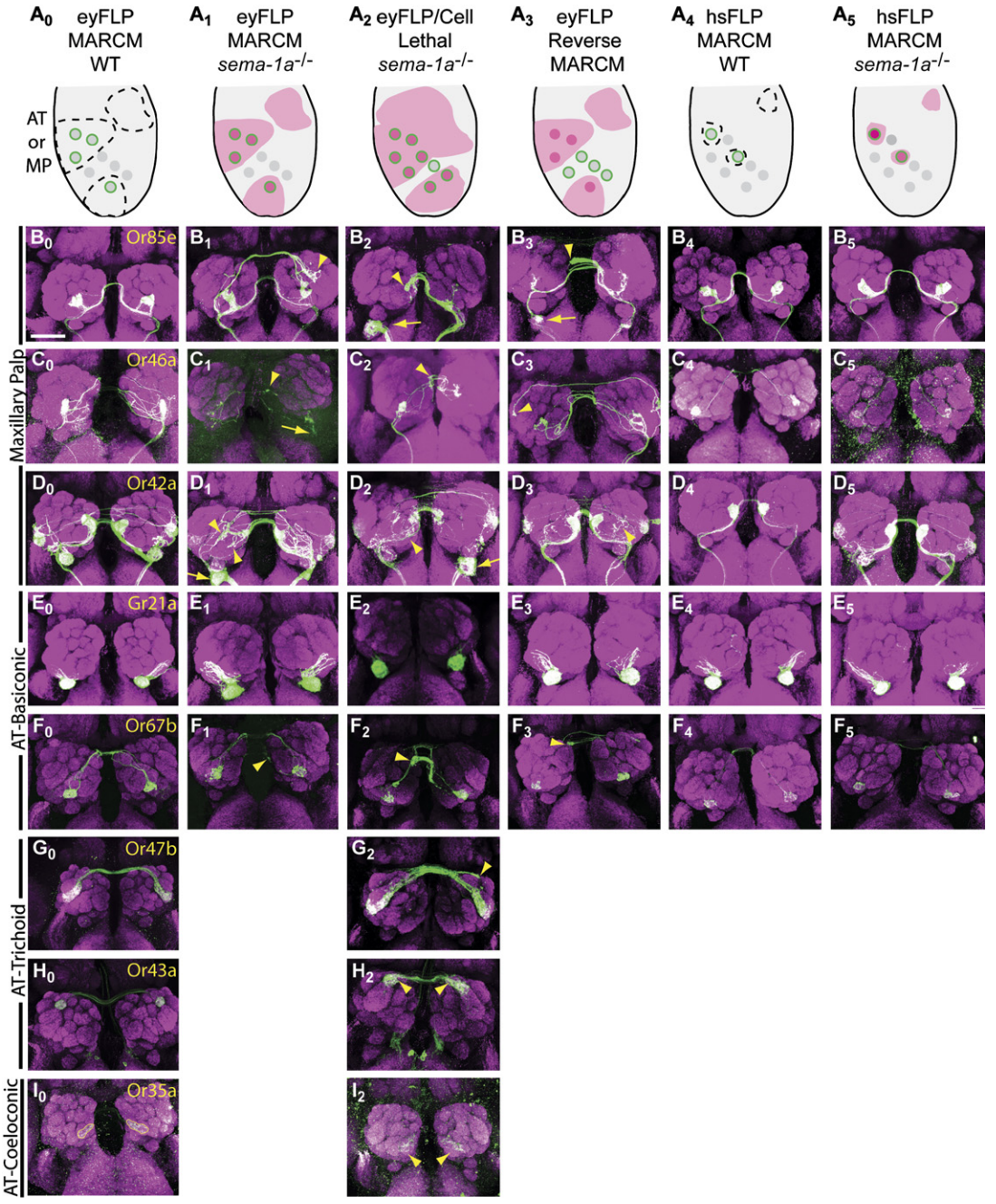

Figure 4. Mosaic Analysis of *sema-1a* in ORN Axon Targeting

(A) A schematic summarizing various mosaic manipulations in the third antennal segment (AT) or maxillary palp (MP). In all conditions, the central brain is heterozygous or wild-type. Circles represent cell bodies of a specific ORN class in the antenna or MP. Green circles indicate labeled ORNs. Dashed regions represent clone borders in control. Pink regions are *sema-1a*$^{-/-}$ clones.

(B–D) Axon targeting of three MP classes as indicated. Arrowheads and arrows indicate respectively intralobe ectopic termination and extralobe terminations.

(E and F) Axon targeting of two antennal basiconic ORN classes as indicated. An example of the 4/5 unaffected basiconic classes, Gr21a targets correctly with *sema-1a* mosaic loss of function. Or67b is the only basiconic class affected by *sema-1a* mosaic loss of function, forming ectopic innervations inside the antennal lobe (arrowheads).

(G–I) Axon targeting of two antennal trichoid and one coeloconic ORN classes as indicated. For all trichoid and coeloconic ORNs, axon mistargeting is shown when the majority of ORNs are mutant for *sema-1a* by the eyFLP/cell lethal strategy. Under other mosaic manipulations, phenotypes are too subtle to score unambiguously. *sema-1a*$^{-/-}$ Or47b ORNs (trichoid) form ectopic innervations (arrowhead). *sema-1a*$^{-/-}$ Or43a ORNs (trichoid) are mildly affected, forming less compact glomerular structures (arrowheads). *sema-1a*$^{-/-}$ Or35a ORNs (coeloconic) similarly are mildly affected (arrowheads). The wild-type Or35a glomerulus is outlined in yellow.

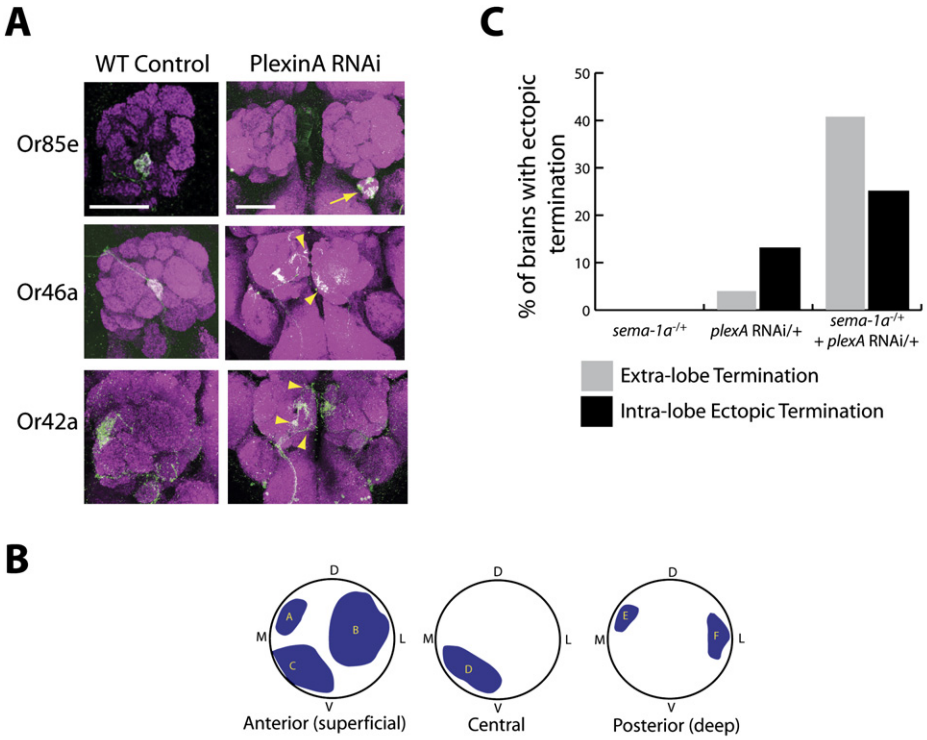

			A	B	C	D	E	F	Other
Or46a	*sema-1a^{P1}*	(15)	0%	13%	80%	27%	33%	13%	
	PlexA RNAi	(16)	50%	0%	63%	25%	63%	19%	
Or85e	*sema-1a^{P1}*	(15)	0%	0%	0%	53%	33%	0%	
	PlexA RNAi	(14)	7%	21%	7%	86%	36%	7%	43% (VC2/DC2)
Or42a	*sema-1a^{P1}*	(13)	0%	31%	15%	46%	46%	0%	
	PlexA RNAi	(17)	0%	18%	0%	59%	24%	0%	18% (VA6,DC2,DA2)
Or42a	0 AT	(9)	44%	56%	33%	56%	33%	11%	22% (VM1, VM6, VL1)

Figure 5. PlexinA as the Sema-1a Receptor in MP Axon Targeting

(A) PlexinA knockdown in ORNs by RNAi results in intra- and extralobe targeting defects similar to *sema-1a* loss-of-function mutants for the three MP ORN classes indicated (see also Figure S5). For WT, only the right antennal lobe is shown at a higher magnification. Arrowheads indicate intralobe ectopic terminations; arrows indicate extralobe terminations. Green, mCD8-GFP marking ORN axons of a given class; magenta, synaptic marker nc82. Scale bar, 50 μm.

(B) Comparison of MP ORN axon mistargeting regions in *sema-1a* mutant (eyFLP/cell lethal), *plexinA* RNAi, and flies devoid of antennal axons as a result of loss of both antennae (0 AT, Figure 2). Data are represented as the percent brains with mistargeting to given regions of the antennal lobe of the total number of brains examined. Frequently mistargeted regions are defined as follows: A: DM5, DM6, DM3; B: VA1lm, VA6, VA7l, VM5; C: VA2, VM2, VM3; D: VC3l, VM4, VA4; E: deep commissural below DM4; F: DL2d, VL2p.

(C) Genetic interaction of *sema-1a* and *plexinA*. Extralobe termination is shown in gray and intralobe ectopic termination is shown in black. Percent extralobe termination = number of brains with extralobe termination/total number of brains examined × 100. n = 62, 71, 93, respectively, for the three genotypes. Percent intralobe ectopic termination = number of brains with intralobe ectopic termination/total number of brains examined × 100. n = 67, 39, 51, respectively, for the three genotypes. For both intra- and extralobe genetic interactions, data are combined from two separate experiments. Experiments were performed at 25°C for extralobe terminations and 18°C for intralobe ectopic terminations.

Genotype: (A) WT: *(pebbled-Gal4); Or-mCD8-GFP.* RNAi: *pebbled-Gal4/+; Or-mCD8-GFP/+; UAS-plexA RNAi/+.* (C) Extralobe termination: *sema-1a^{P1}/+; (UAS-plexA RNAi, TM6b)/+. pebbled-Gal4, UAS-mCD8GFP; CyO/+; UAS-plexA RNAi/+. pebbled-Gal4, UAS-mCD8GFP; sema-1a^{P1}/+; UAS-plexA RNAi/+.* Intralobe ectopic termination: *sema-1a^{P1}/+; Or46a-mCD8-GFP/(Tm6B/UAS-plexA RNAi). pebbled-Gal4/+; CyO/+; Or46a-mCD8GFP/UAS-plexA RNAi. pebbled-Gal4/+; sema-1a^{P1}/+; Or46a-mCD8GFP/UAS-plexA RNAi.*

act in the same pathway. Notably, the defined six regions are also frequently mistargeted by MP ORNs in the absence of antennal ORNs (Figures 2B$_2$ and 2B$_3$; quantified in Figure 5B), consistent with the notion that Sema-1a/PlexinA signaling might be a major component of antennal-MP axon-axon interactions.

Green, mCD8-GFP marking ORN axons of a given class; magenta, synaptic marker nc82. Scale bar, 50 μm. Genotype: (A$_0$) *eyFLP UAS-mCD8GFP; FRT40a/tubP-G80 FRT40a; Or-Gal4/+.* (A$_1$) *eyFLP UAS-mCD8GFP; sema-1a^{P1} FRT40a/tubP-G80 FRT40a; Or-Gal4/+.* (A$_2$) *eyFLP UAS-mCD8GFP; sema-1a^{P1} FRT40a/cycE FRT40a; Or-Gal4/+.* (A$_3$) *eyFLP UAS-mCD8GFP; tubP-G80 sema-1a^{P1} FRT40a/FRT40a; Or-Gal4/+.* (A$_4$) *hsFLP UAS-mCD8GFP; FRT40a/ tubP-G80 FRT40a; Or-Gal4/+.* (A$_5$) *hsFLP UAS-mCD8GFP; sema-1a^{P1} FRT40a/tubP-G80 FRT40a; Or-Gal4/+.*

Basiconic classes of ORNs from the antenna, which do not require Sema-1a for axon targeting, displayed targeting defects in *plexinA* RNAi experiments (Figure S5, arrowheads). This is consistent with our finding that antennal axons also express PlexinA (Figures 3D and 3E). In addition, PlexinA knockdown in some cases caused more frequent mistargeting of MP axons than Sema-1a loss-of-function (Figure 5B, bottom). Thus, in addition to being a receptor for ORN-derived Sema-1a, PlexinA may be a receptor for non-ORN-derived Sema-1a or may have additional ligands in the olfactory system such as other Semaphorins (Winberg et al., 1998; Ayoob et al., 2006).

Due to the fourth chromosome location of the *plexinA* gene, we cannot perform conventional mosaic analysis. In addition, the lack of MP-specific Gal4 line during early pupal development prevented us from directly confirming PlexinA's requirement in MP axons. Therefore, we tested the genetic interactions between Sema-1a and PlexinA to provide additional support for PlexinA's function as the receptor for Sema-1a in MP ORN axon targeting.

sema-1a and *plexinA* Exhibit Strong Genetic Interactions in MP Axon Targeting

Ligands and receptors in *Drosophila* often exhibit dosage-sensitive genetic interactions (Artavanis-Tsakonas et al., 1995; Winberg et al., 1998; Kidd et al., 1999). We tested for potential genetic interactions between *sema-1a* and *plexinA* using both extralobe terminations and intralobe ectopic terminations of MP axons as quantitative assays. We found that reduction of the Sema-1a level by half (*sema-1a*$^{+/-}$) did not result in any phenotypes. Reduction of the PlexinA level specifically in ORNs using *pebbled*-Gal4, UAS-*plexinA* RNAi resulted in phenotypes of low frequency at a low temperature. However, combination of these genetic manipulations resulted in a marked increase in frequency of both phenotypes (Figure 5C). Although genetic interaction studies by themselves do not prove that two genes work in the same pathway, they nevertheless provide additional support for a ligand-receptor relationship between Sema-1a and PlexinA in the context of MP axon targeting.

Two Distinct Mechanisms of Sema-1a-Mediated Axon-Axon Interactions

So far we have presented evidence that Sema-1a-PlexinA signaling mediates axon-axon interactions essential for ORN axon targeting but have not yet resolved the cellular basis for these interactions. Specifically, the Sema-1a signal required for MP axon targeting could originate from other MP axons, antennal axons, or both, on the ipsi- or contralateral side. To distinguish between these possibilities, we needed a means to selectively eliminate Sema-1a function from either the antenna or the maxillary palp and to distinguish between ipsi- and contralateral MP axons. No genetic elements have yet been reported that would allow us to drive mitotic recombination or transgene expression selectively in early antenna or maxillary palp. However, in the course of the eyFLP *sema-1a* MARCM experiments, we occasionally observed individual flies that do not have any eyFLP MARCM clones in one or both maxillary palps, whereas every antenna always has abundant clones of various sizes. This could be because of the smaller number of cells in the maxillary palp and/or the more transient expression of *eyeless* in the maxillary palp (Dominguez and Casares, 2005). Regardless of the cause, these flies provided a strategy to dissect the contributions of Sema-1a on antennal and maxillary palp ORN axons to MP axon targeting.

In our experimental design (Figure 6A), we labeled *sema-1a*$^{-/-}$ eyFLP MARCM clones with UAS-myr-mRFP (available through the Bloomington Stock Center after contribution from H. Chang) and visualized axon targeting from a single class of MP ORNs with a direct Or46a promoter-driven mCD8-GFP (Couto et al., 2005). We separately collected flies that have *sema-1a*$^{-/-}$ eyFLP MARCM clones in 2 MPs (Figure 6A$_1$), 0 MP (Figure 6A$_2$), or 1 MP (Figures 6A$_3$ and 6A$_4$) based on RFP fluorescence in the maxillary palp cell bodies. For flies with 1 MP, we further separated them into two groups. In one group, we unilaterally severed the MP without clones (Figure 6A$_3$; 1MPΔWT); in the other, we severed the MP with clones (Figure 6A$_4$; 1MPΔmutant). In both cases, we then allowed the severed axons to degenerate before processing for phenotypic analysis. Using this strategy, we could selectively examine Or46a axons originating from the remaining mutant (1MPΔWT) or wild-type (1MPΔmutant) MP. There was no obvious difference in clone sizes in the antenna across the four groups (data not shown).

We already know from eyFLP *sema-1a*$^{-/-}$ experiments described earlier (Figure 4C$_1$; Table 1) that Or46a ORN axons exhibit two distinct types of targeting errors: intralobe ectopic terminations and extralobe terminations. If MP axon targeting exclusively requires antennal Sema-1a, then all four groups should exhibit the same phenotypes (since antennae contain *sema-1a*$^{-/-}$ clones of a similar size in all cases). If MP axon targeting exclusively requires Sema-1a-mediated MP-MP axon interactions, then the 0MP group should not exhibit any phenotypes (since all MP axons are heterozygous for *sema-1a*). Furthermore, if MP-MP axon interactions do indeed contribute to MP axon targeting, then by comparing the phenotypes from 1MPΔWT and 1MPΔmutant groups, we can resolve whether these interactions occur between ipsilateral or contralateral MP axons. For example, if Sema-1a-mediated MP-MP interactions are exclusively between ipsilateral axons and there is no contribution of contralateral axons, then MP axons in the 1MPΔmutant group should have the same phenotype as the 0MP group; if contralateral interactions are involved, the 1MPΔmutant group should have more severe phenotypes than the 0MP group.

We scored Or46a MP axon mistargeting blindly for these four experimental groups. The results are shown as representative images in Figure 6B and quantified in Figure 6C. Interestingly, the extralobe termination phenotype is found exclusively in 2MP and in 1MPΔWT groups, but never in 0MP or 1MPΔmutant groups. These data indicate that

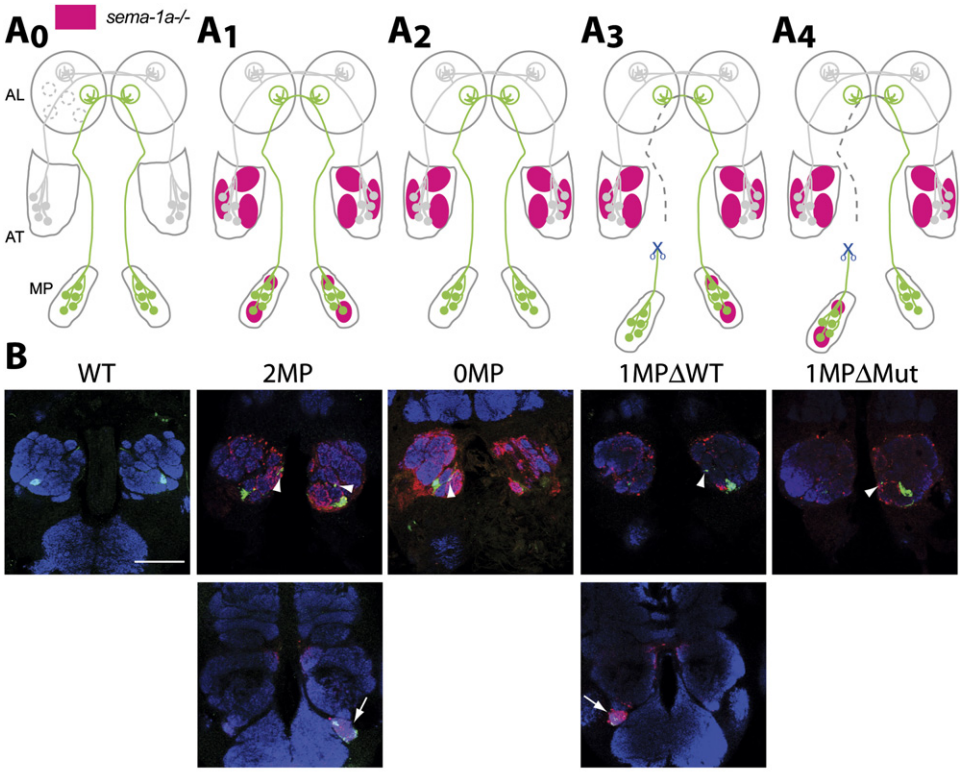

		Intra-lobe Ectopic Termination	A	B	C	D	E	F	Extra-lobe Termination
WT	(17)	23%	0%	6%	12%	6%	6%	0%	0%
2MP	(45)	80%	31%	2%	71%	38%	11%	4%	12%
0MP	(24)	83%	8%	0%	75%	25%	0%	0%	0%
1MPΔWT	(11)	100%	36%	9%	45%	27%	18%	0%	27%
1MPΔMut	(16)	94%	25%	0%	75%	56%	6%	0%	0%

Figure 6. Cellular Bases of Sema-1a-Mediated Axon-Axon Interactions

(A_0–A_4) Schematic of experimental design to test the contributions of various forms of axon-axon interactions to MP axon targeting (see text for detail).

(B) Representative images of axon targeting of Or46a ORN from the maxillary palp. Top row, intralobe ectopic terminations indicated by white arrowheads. Bottom row, extralobe terminations indicated by white arrows. Note for all images a single section of the antennal lobe is shown (top row, anterior; bottom row, posterior below ALs, thus nc82 staining is weaker). The amount of red *sema-1a*$^{-/-}$ axons is equivalent across 0MP, 1MP, and 2MP groups (data not shown); however, this is not reflected in single sections of the AL shown here, as many red axons are not in these planes. For 1 MP groups (A_3 and A_4), MPs were cut 5–8 days prior to dissection. Green, Or46a axons visualized by Or46a-mCD8-GFP; red, myr-mRFP marker for *sema-1a*$^{-/-}$ eyFLP MARCM clones; blue: nc82. Scale bar, 50 μm.

(C) Quantification of intralobe ectopic termination as well as extralobe termination for different clone types. All quantification was done blindly. Intralobe ectopic termination frequency = percent of total brains with intralobe ectopic termination. Regional quantification of intralobe ectopic termination = percent of total brains with ectopic terminations in regions indicated (see Figure 5 legend for region definition). Extralobe termination = percent of MP bundles that terminate outside the AL (number of MP axon bundles that terminate outside the AL/total number of MP axon bundles examined × 100). The number of brains examined is indicated in parentheses.

Genotype: WT: *elav-Gal4, eyFLP; tubP-G80 FRT40a or sema-1a*^{P1} *FRT40a/CyO; UAS-myr-mRFP/Or46a-mCD8-GFP.* 2 MP, 1 MP, 0 MP: *elav-Gal4, eyFLP; sema-1a*^{P1} *FRT 40a/tubP-G80 FRT 40a; UAS-myr-mRFP/Or46a-mCD8-GFP.*

the extralobe termination is exclusively contributed by Sema-1a-mediated ipsilateral MP-MP interactions. This interpretation is consistent with our finding that in the absence of all antennal axons (Figure 2), we did not observe extralobe termination of MP axons (data not shown) despite their mistargeting defects within the antennal lobe.

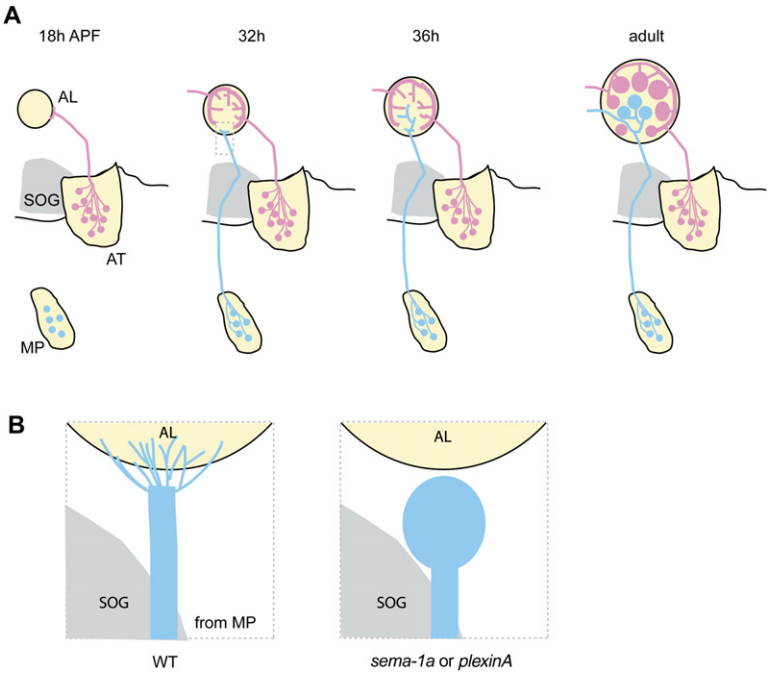

Figure 7. A Model for Temporal Target Restriction

(A) Axons of antennal ORNs (pink) arrive at the developing antennal lobe (circle) at 18 hr APF and start to invade the lobe by 32 hr APF. Axons of the MP ORNs (blue) begin to reach the antennal lobe at 32 hr APF. Through Sema-1a-PlexinA-mediated repulsion, MP axons are constrained to their appropriate target glomeruli by Sema-1a expressed on antennal ORN axons. AT, antenna; MP, maxillary palp; AL, antennal lobe; SOG, suboesophageal ganglion (shaded in gray). Not drawn to scale. (B) Magnified schematic of WT MP ORN axon bundle (blue) innervating the AL (yellow circle) at 32 hr APF (left, similar area as dotted box in [A] at 32 hr APF). In *sema-1a* or *plexinA* mutants, the MP axons instead terminate between the AL and the SOG (right box) as a result of lack of defasciculation.

A very different picture emerges when we examined the intralobe ectopic termination. Here, Or46a axon mistargeting occurs in all four experimental groups (Figure 6B). Given the mosaic nature of these experiments that introduces large variance in clone location, quantitative statistical comparisons are difficult. However, tabulation of the frequency and location of intralobe ectopic terminations (Figure 6C) reveals no obvious difference among the four groups. This experiment therefore indicates that correct targeting of MP Or46a axons within the antennal lobe depends on Sema-1a predominantly, if not exclusively, on antennal axons.

DISCUSSION

Temporal Target Restriction of ORN Axons Mediated by Sema-1a/PlexinA

Previous genetic mosaic analyses of the POU transcription factor Acj6 suggested hierarchical interactions among different classes of ORNs contribute to their axon targeting (Komiyama et al., 2004). However, it was unclear what molecules mediate these interactions and under what cellular and developmental context these interactions take place. In this study, we provided mechanisms to address both questions. We propose a "temporal target restriction" model (Figure 7A). Antennal ORN axons reach and start to pattern the developing antennal lobe before the arrival of MP axons. These early-arriving antennal axons express a high level of Sema-1a. Late-arriving MP axons express the repulsive receptor PlexinA and are repelled by Sema-1a expressed on the antennal axons. Thus, antennal ORN axons restrict MP ORN axon targeting to the proper antennal lobe region. The target glomeruli of MP classes are indeed clustered in a small area in the adult antennal lobe, surrounded by target glomeruli of antennal ORNs (Couto et al., 2005).

Multiple lines of evidence support the temporal target-restriction model. First, pioneering axons of the antennal ORNs reach the antennal lobe ~12 hr prior to those of the MP ORNs (Figure 1). Second, loss of antennal ORN axons results in mistargeting of MP axons, but not vice versa (Figure 2). Third, both Sema-1a and its known receptor PlexinA are expressed in ORN axons at appropriate developmental stages (Figure 3). Fourth, extensive genetic mosaic analyses of *sema-1a* indicate that Sema-1a is required for axon targeting of all MP ORN classes and acts non-cell-autonomously as a ligand (Figure 4; Table 1). Fifth, knockdown of PlexinA in ORNs results in MP mistargeting phenotypes similar to those of *sema-1a* mosaics and those resulting from loss of antennal axons (Figure 5). Lastly, MP axon targeting within the antennal lobe predominantly relies on Sema-1a on antennal axons (Figure 6).

This model makes a few additional predictions that we have not directly tested due to technical limitations: (1) PlexinA should act cell autonomously in MP ORNs; (2) Sema-1a/PlexinA should mediate repulsion between antennal and MP axons; (3) the sequential arrival of antennal and MP axon innervation should be essential for their interactions. The first prediction is supported by previous findings that PlexinA acts as a receptor for Sema-1a in embryonic motor axon guidance (Winberg et al., 1998), as well as our own data that PlexinA acts in ORNs and genetically interacts with Sema-1a. The second prediction is suggested by MP axon mistargeting to normal targets of antennal axons in *sema-1a*$^{-/-}$ and *plexinA* RNAi conditions and is consistent with the well-documented repulsive

functions of Sema-1a in *Drosophila* embryos (Winberg et al., 1998; Yu et al., 1998) and of Semaphorins more generally from insects to mammals (Tessier-Lavigne and Goodman, 1996; Dickson, 2002). Finally, the temporal evidence remains correlative rather than causal, since it is currently not possible to specifically alter the sequence of axon arrival.

Although a central focus of our study is the axon-axon interaction between antennal and MP ORNs, it is likely that similar axon-axon interactions take place between different classes of antennal axons to regulate their targeting. The following data from our study support this extrapolation. Antennal ORN axons express both Sema-1a and PlexinA; certain classes of antennal ORN axons require Sema-1a non-cell-autonomously (Figure 4; Table 1); and PlexinA is required for proper targeting of many antennal ORN classes examined. A rigorous test of this extrapolation will require the identification of ORN class-specific promoters that are expressed early during development. This will allow for the examination of axon arrival timing and genetic manipulations of specific antennal ORN classes.

Contribution of Axon-Axon Interactions to *Drosophila* ORN Axon Targeting

Axon-axon interactions among ORN axons likely represent one of multiple mechanisms that enable ~50 classes of ORNs to target their axons to ~50 glomeruli. In the phenotypic analyses described here for *sema-1a* and *plexinA*, although the severity of phenotypes varies depending on classes and genetic manipulations, the normal glomerular targets are often still innervated. This could be rationalized by the mosaic nature of *sema-1a* loss-of-function analyses, the partial knockdown of PlexinA by RNAi, or contributions of other ligand-receptor pairs to antenna-MP axon-axon interactions. However, even in the extreme cases of *smo* clones where both antennae fail to develop and all antennal axons are presumably missing, the MP axon mistargeting phenotype is only partially penetrant. These observations suggest that axon-axon interactions contribute to the fidelity of axon targeting together with other mechanisms. We envision that global cues expressed in the antennal lobe act first to direct pioneering ORN axons to different general areas of the antennal lobe, axon-axon interactions then act to constrain the coarse targeting of later-arriving axons, and pre- and postsynaptic recognition (Zhu et al., 2006) contributes to the final target selection.

Multiple Functions of Sema-1a in the *Drosophila* Olfactory System Development

Our genetic mosaic analyses indicate that Sema-1a- and PlexinA-mediated axon-axon interactions are also used among MP axons to regulate their entry into the antennal lobe. A disruption of MP-MP interactions results in occasional MP axon termination before entering the antennal lobe (Figure 7B). This phenotype is quite analogous to the failure of motor axons to defasciculate from their fascicles upon reaching their muscle field observed in *sema-1a* or *plexinA* mutant *Drosophila* embryos (Winberg et al., 1998; Yu et al., 1998); this embryonic phenotype has been interpreted as a defect in Sema-1a-PlexinA mediated axon-axon repulsion, which normally would facilitate defasciculation of individual axons from the rest of the fascicle. Similarly, MP-MP axon-axon repulsion mediated by Sema-1a and PlexinA may serve to loosen the individual MP axons within the bundle, allowing them to dissociate from each other and facilitate their entry into the antennal lobe (Figure 7B).

In a separate study, we show that at an earlier stage during development, Sema-1a acts cell autonomously as a receptor (in response to an unknown ligand) in olfactory PNs for their dendritic targeting (Komiyama et al., 2007). It is thus of interest that Sema-1a acts in two different modes to regulate targeting specificity of PNs and ORNs that eventually become synaptic partners. This finding also raises the possibility that in addition to acting as a receptor for PN dendritic targeting, Sema-1a on PN dendrites might also act as a ligand for targeting of ORN axons that express and require PlexinA. However, our preliminary studies (T.K. and L.L., unpublished data) have not yielded positive evidence to support this hypothesis.

Semaphorins and their receptors have various functions in wiring the nervous system (Tessier-Lavigne and Goodman, 1996; Dickson, 2002), including olfactory systems. In mice, Semaphorin3F-Neuropilin2 signaling restricts ORN axon termination to the glomerular layer, preventing axon overshoot into deeper layers of the olfactory bulb (Cloutier et al., 2002, 2004; Walz et al., 2002). Moreover, Semaphorin3A-Neuropilin1 contributes to the broad organization of ORN axon targeting (Schwarting et al., 2000, 2004; Walz et al., 2002). Semaphorin3A, expressed in a broad compartment of the olfactory bulb by glial cells, repels Neuropilin1-expressing ORNs from this area. Sema3A-Neuropilin1 signaling has a different function in chick ORN targeting: it prevents ORNs from prematurely entering, and subsequently overshooting, the olfactory bulb (Renzi et al., 2000). Our findings are conceptually and qualitatively distinct from these previous reports: we find that Sema-1a mediates the interactions between axons with temporally distinct innervation patterns, rather than the interaction between axons and their targets.

Axon-Axon Interaction and Temporal Target Restriction in Neuronal Wiring

Clear examples that temporal sequence plays an important role in neuronal wiring come from numerous studies on pioneering axons from insects to mammals. Early axons lay down the path for late ones to follow, presumably through axon-axon adhesion and fasciculation (Bate, 1976; Raper et al., 1983; Eisen et al., 1989; McConnell et al., 1989; Lin et al., 1995 and references therein). Axon-axon interactions have also been proposed to play a role in final target selection. For example, in *Drosophila* photoreceptor axon targeting, R1–R6 axons from the same ommatidium, upon reaching the laminar layer,

select six distinct cartridges to send their final terminal branches. Hierarchical interactions among photoreceptors contribute to their target selections, although the mechanism is unknown (Clandinin and Zipursky, 2000). In the establishment of the retinotopic map of the vertebrate visual system, relative rather than absolute EphA receptor levels on retinal ganglion cells determine the anterior-posterior positions of their axon termination at the target, likely through axon-axon interactions and competition (Brown et al., 2000). In mouse ORN axon targeting, axon-axon interactions have been proposed to allow ORNs expressing the same OR to converge and stabilize (Ebrahimi and Chess, 2000; Feinstein and Mombaerts, 2004) and to provide comparisons and discriminations of different ORN classes (Feinstein and Mombaerts, 2004). The mechanisms by which these axon-axon interactions regulate targeting specificity are not well understood, and the role of temporal sequences has not been explored in these systems. A difficulty is to unravel where these neurons interact—at cell bodies, axon paths, or target areas. The *Drosophila* olfactory system provides an excellent model to explore the molecular and cellular basis of these axon-axon interactions. In particular, the physical separation of ORN cell bodies into two sensory organs, the antenna and the maxillary palp, allows us to assess afferent-afferent interactions exclusively at their final target area—a feature we have exploited here to dissect the cellular and molecular basis of ORN axon-axon interactions.

Examples of a common target area innervated by multiple input axons—whether arriving simultaneously or sequentially—are ample in developing nervous systems. We propose that target restriction through axon-axon interactions as described here could contribute widely to establishing neuronal wiring specificity.

EXPERIMENTAL PROCEDURES

Mosaic Analysis

MARCM analysis was performed according to previously described methods (Lee and Luo, 1999; Komiyama et al., 2004). *sema-1a*^{P1} and *sema-1a*^{P2} are null and strong hypomorphic alleles of *sema-1a*, respectively (Yu et al., 1998). *smo*^{3} is a null allele of *smoothened* (Chen and Struhl, 1998).

Immunostaining

Immunostaining was performed according to previously described methods (Komiyama et al., 2003). Rabbit anti-Sema-1a (kind gift of A. Kolodkin) was used at 1:5000. Rabbit anti-PlexinA antibodies were generated by New England Peptide according to the peptide sequence SDKNEKSHKYETLNISKC in the cytoplasmic domain of the PlexinA protein, custom affinity-purified, and used at 1:500.

Transgenes

Or-Gal4s were described previously (Hummel et al., 2003; Hummel and Zipursky, 2004; Komiyama et al., 2004; Couto et al., 2005; Fishilevich and Vosshall, 2005; Kreher et al., 2005). UAS-RNAi for *sema-1a* and *plexinA* were part of a whole-genome transgenic RNAi library (G. Dietzl and B.J.D., unpublished data). *pebbled*-Gal4 was identified from an expression screen of newly generated Gal4 enhancer trap lines (U. Heberlein, E.C. Marin, and L.L., unpublished data) and mapped to the *pebbled* locus using inverse PCR. UAS-HA-synaptotagmin was as described (Robinson et al., 2002). Or-mCD8GFP transgenes were as described (Couto et al., 2005).

Supplemental Data

The Supplemental Data for this article can be found online at http://www.neuron.org/cgi/content/full/53/2/185/DC1/.

ACKNOWLEDGMENTS

We are grateful to E.C. Marin, U. Heberlein, and G. Dietzl for sharing unpublished reagents; J.R. Carlson, S.L. Zipursky, L.B. Vosshall, A.L. Kolodkin, E. Buchner and their lab members, and the Bloomington Stock Center for other reagents; K. Shen, T. Clandinin, D. Manoli, and members of the Luo lab for comments and discussions. Supported by a fellowship from Developmental and Neonatal Training Program (L.B.S.), Japan Stanford Association (T.K.), a Human Frontier Science Program Organization postdoctoral fellowship (D.B.), funding from Boehringer Ingelheim (A.C. and B.J.D.), and an NIH grant (R01-DC005982 to L.L.). L.L. is an investigator of the Howard Hughes Medical Institute.

Received: July 24, 2006
Revised: September 19, 2006
Accepted: December 1, 2006
Published: January 17, 2007

REFERENCES

Ang, L.H., Kim, J., Stepensky, V., and Hing, H. (2003). Dock and Pak regulate olfactory axon pathfinding in Drosophila. Development *130*, 1307–1316.

Artavanis-Tsakonas, S., Matsuno, K., and Fortini, M.E. (1995). Notch signaling. Science *268*, 225–232.

Ayoob, J.C., Terman, J.R., and Kolodkin, A.L. (2006). Drosophila Plexin B is a Sema-2a receptor required for axon guidance. Development *133*, 2125–2135.

Bate, C.M. (1976). Pioneer neurones in an insect embryo. Nature *260*, 54–56.

Berdnik, D., Chihara, T., Couto, A., and Luo, L. (2006). Wiring stability of the adult Drosophila olfactory circuit after lesion. J. Neurosci. *26*, 3367–3376.

Brown, A., Yates, P.A., Burrola, P., Ortuno, D., Vaidya, A., Jessell, T.M., Pfaff, S.L., O'Leary, D.D., and Lemke, G. (2000). Topographic mapping from the retina to the midbrain is controlled by relative but not absolute levels of EphA receptor signaling. Cell *102*, 77–88.

Cafferty, P., Yu, L., Long, H., and Rao, Y. (2006). Semaphorin-1a functions as a guidance receptor in the Drosophila visual system. J. Neurosci. *26*, 3999–4003.

Chen, Y., and Struhl, G. (1998). In vivo evidence that Patched and Smoothened constitute distinct binding and transducing components of a Hedgehog receptor complex. Development *125*, 4943–4948.

Cho, K.O., Chern, J., Izaddoost, S., and Choi, K.W. (2000). Novel signaling from the peripodial membrane is essential for eye disc patterning in *Drosophila*. Cell *103*, 331–342.

Clandinin, T.R., and Zipursky, S.L. (2000). Afferent growth cone interactions control synaptic specificity in the *Drosophila* visual system. Neuron *28*, 427–436.

Cloutier, J.F., Giger, R.J., Koentges, G., Dulac, C., Kolodkin, A.L., and Ginty, D.D. (2002). Neuropilin-2 mediates axonal fasciculation, zonal segregation, but not axonal convergence, of primary accessory olfactory neurons. Neuron *33*, 877–892.

Cloutier, J.F., Sahay, A., Chang, E.C., Tessier-Lavigne, M., Dulac, C., Kolodkin, A.L., and Ginty, D.D. (2004). Differential requirements for semaphorin 3F and Slit-1 in axonal targeting, fasciculation, and segregation of olfactory sensory neuron projections. J. Neurosci. *24*, 9087–9096.

Couto, A., Alenius, M., and Dickson, B.J. (2005). Molecular, anatomical, and functional organization of the *Drosophila* olfactory system. Curr. Biol. *15*, 1535–1547.

de Bruyne, M., Clyne, P.J., and Carlson, J.R. (1999). Odor coding in a model olfactory organ: the Drosophila maxillary palp. J. Neurosci. *19*, 4520–4532.

de Bruyne, M., Foster, K., and Carlson, J.R. (2001). Odor coding in the *Drosophila* antenna. Neuron *30*, 537–552.

Dickson, B.J. (2002). Molecular mechanisms of axon guidance. Science *298*, 1959–1964.

Dobritsa, A.A., van der Goes van Naters, W., Warr, C.G., Steinbrecht, R.A., and Carlson, J.R. (2003). Integrating the molecular and cellular basis of odor coding in the *Drosophila* antenna. Neuron *37*, 827–841.

Dominguez, M., and Casares, F. (2005). Organ specification-growth control connection: new in-sights from the Drosophila eye-antennal disc. Dev. Dyn. *232*, 673–684.

Ebrahimi, F.A., and Chess, A. (2000). Olfactory neurons are interdependent in maintaining axonal projections. Curr. Biol. *10*, 219–222.

Eisen, J.S., Pike, S.H., and Debu, B. (1989). The growth cones of identified motoneurons in embryonic zebrafish select appropriate pathways in the absence of specific cellular interactions. Neuron *2*, 1097–1104.

Feinstein, P., and Mombaerts, P. (2004). A contextual model for axonal sorting into glomeruli in the mouse olfactory system. Cell *117*, 817–831.

Fishilevich, E., and Vosshall, L.B. (2005). Genetic and functional subdivision of the *Drosophila* antennal lobe. Curr. Biol. *15*, 1548–1553.

Hallem, E.A., and Carlson, J.R. (2006). Coding of odors by a receptor repertoire. Cell *125*, 143–160.

Hummel, T., and Zipursky, S.L. (2004). Afferent induction of olfactory glomeruli requires N-cadherin. Neuron *42*, 77–88.

Hummel, T., Vasconcelos, M.L., Clemens, J.C., Fishilevich, Y., Vosshall, L.B., and Zipursky, S.L. (2003). Axonal targeting of olfactory receptor neurons in *Drosophila* is controlled by Dscam. Neuron *37*, 221–231.

Imai, T., Suzuki, M., and Sakano, H. (2006). Odorant receptor-derived cAMP signals direct axonal targeting. Science *314*, 657–661.

Jefferis, G.S., Marin, E.C., Stocker, R.F., and Luo, L. (2001). Target neuron prespecification in the olfactory map of Drosophila. Nature *414*, 204–208.

Jefferis, G.S., Vyas, R.M., Berdnik, D., Ramaekers, A., Stocker, R.F., Tanaka, N., Ito, K., and Luo, L. (2004). Developmental origin of wiring specificity in the olfactory system of *Drosophila*. Development *131*, 117–130.

Jhaveri, D., Sen, A., Reddy, G.V., and Rodrigues, V. (2000). Sense organ identity in the Drosophila antenna is specified by the expression of the proneural gene atonal. Mech. Dev. *99*, 101–111.

Jhaveri, D., Saharan, S., Sen, A., and Rodrigues, V. (2004). Positioning sensory terminals in the olfactory lobe of Drosophila by Robo signaling. Development *131*, 1903–1912.

Kidd, T., Bland, K.S., and Goodman, C.S. (1999). Slit is the midline repellent for the robo receptor in *Drosophila*. Cell *96*, 785–794.

Kolodkin, A.L., Matthes, D.J., and Goodman, C.S. (1993). The semaphorin genes encode a family of transmembrane and secreted growth cone guidance molecules. Cell *75*, 1389–1399.

Komiyama, T., and Luo, L. (2006). Development of wiring specificity in the olfactory system. Curr. Opin. Neurobiol. *16*, 67–73.

Komiyama, T., Johnson, W.A., Luo, L., and Jefferis, G.S. (2003). From lineage to wiring specificity. POU domain transcription factors control precise connections of *Drosophila* olfactory projection neurons. Cell *112*, 157–167.

Komiyama, T., Carlson, J.R., and Luo, L. (2004). Olfactory receptor neuron axon targeting: intrinsic transcriptional control and hierarchical interactions. Nat. Neurosci. *7*, 819–825.

Komiyama, T., Sweeney, L.B., Schuldiner, O., Garcia, K.C., and Luo, L. (2007). Dendritic targeting of olfactory projection neurons directed by cell-autonomous action of a Semaphorin-1a gradient. Cell, in press.

Kreher, S.A., Kwon, J.Y., and Carlson, J.R. (2005). The molecular basis of odor coding in the *Drosophila* larva. Neuron *46*, 445–456.

Lee, T., and Luo, L. (1999). Mosaic analysis with a repressible cell marker for studies of gene function in neuronal morphogenesis. Neuron *22*, 451–461.

Lin, D.M., Auld, V.J., and Goodman, C.S. (1995). Targeted neuronal cell ablation in the *Drosophila* embryo: Pathfinding by follower growth cones in the absence of pioneers. Neuron *14*, 707–715.

McConnell, S.K., Ghosh, A., and Shatz, C.J. (1989). Subplate neurons pioneer the first axon pathway from the cerebral cortex. Science *245*, 978–982.

Mombaerts, P., Wang, F., Dulac, C., Chao, S.K., Nemes, A., Mendelsohn, M., Edmondson, J., and Axel, R. (1996). Visualizing an olfactory sensory map. Cell *87*, 675–686.

Newsome, T.P., Asling, B., and Dickson, B.J. (2000). Analysis of Drosophila photoreceptor axon guidance in eye-specific mosaics. Development *127*, 851–860.

Raper, J.A., Bastiani, M., and Goodman, C.S. (1983). Pathfinding by neuronal growth cones in grasshopper embryos. II. Selective fasciculation onto specific axonal pathways. J. Neurosci. *3*, 31–41.

Renzi, M.J., Wexler, T.L., and Raper, J.A. (2000). Olfactory sensory axons expressing a dominant-negative semaphorin receptor enter the CNS early and overshoot their target. Neuron *28*, 437–447.

Robinson, I.M., Ranjan, R., and Schwarz, T.L. (2002). Synaptotagmins I and IV promote transmitter release independently of Ca(2+) binding in the C(2)A domain. Nature *418*, 336–340.

Schwarting, G.A., Kostek, C., Ahmad, N., Dibble, C., Pays, L., and Puschel, A.W. (2000). Semaphorin 3A is required for guidance of olfactory axons in mice. J. Neurosci. *20*, 7691–7697.

Schwarting, G.A., Raitcheva, D., Crandall, J.E., Burkhardt, C., and Puschel, A.W. (2004). Semaphorin 3A-mediated axon guidance regulates convergence and targeting of P2 odorant receptor axons. Eur. J. Neurosci. *19*, 1800–1810.

Stocker, R.F. (1994). The organization of the chemosensory system in Drosophila melanogaster: a review. Cell Tissue Res. *275*, 3–26.

Terman, J.R., Mao, T., Pasterkamp, R.J., Yu, H.H., and Kolodkin, A.L. (2002). MICALs, a family of conserved flavoprotein oxidoreductases, function in plexin-mediated axonal repulsion. Cell *109*, 887–900.

Tessier-Lavigne, M., and Goodman, C.S. (1996). The molecular biology of axon guidance. Science *274*, 1123–1133.

Walz, A., Rodriguez, I., and Mombaerts, P. (2002). Aberrant sensory innervation of the olfactory bulb in neuropilin-2 mutant mice. J. Neurosci. *22*, 4025–4035.

Wang, F., Nemes, A., Mendelsohn, M., and Axel, R. (1998). Odorant receptors govern the formation of a precise topographic map. Cell *93*, 47–60.

Winberg, M.L., Noordermeer, J.N., Tamagnone, L., Comoglio, P.M., Spriggs, M.K., Tessier-Lavigne, M., and Goodman, C.S. (1998). Plexin A is a neuronal semaphorin receptor that controls axon guidance. Cell *95*, 903–916.

Yu, H.H., Araj, H.H., Ralls, S.A., and Kolodkin, A.L. (1998). The transmembrane Semaphorin Sema I is required in *Drosophila* for embryonic motor and CNS axon guidance. Neuron *20*, 207–220.

Zhu, H., and Luo, L. (2004). Diverse functions of N-cadherin in dendritic and axonal terminal arborization of olfactory projection neurons. Neuron *42*, 63–75.

Zhu, H., Hummel, T., Clemens, J.C., Berdnik, D., Zipursky, S.L., and Luo, L. (2006). Dendritic patterning by Dscam and synaptic partner matching in the Drosophila antennal lobe. Nat Neurosci. *9*, 349–355.